

# MODELING OF STRESS DISTRIBUTIONS ON THE MICROSTRUCTURAL LEVEL IN ALLOY 600

Krzysztof J. Kozaczek

Oak Ridge National Laboratory

Oak Ridge, TN 37831-6064

Bojan G. Petrovic and Clayton O. Ruud

The Pennsylvania State University

University Park, PA 16802

Allan R. McIlree

Electric Power Research Institute

Palo Alto, CA 94304-1395

## ABSTRACT

The stress distribution in a random polycrystalline material (Alloy 600) was studied using a topologically correct microstructural model. The distributions of von Mises and hydrostatic stresses at the grain vertices, which could be important factors when studying the intergranular stress corrosion cracking, were analyzed as a function of microstructure, grain orientations and loading conditions. The grain size, shape, and orientation had a more pronounced effect on stress distribution than the loading conditions. At grain vertices the stress concentration factor was higher for hydrostatic stress (1.7) than for von Mises stress (1.5). The stress /strain distribution in the volume (grain interiors) is a normal distribution and does not depend on the location of the studied material volume i.e., surface vs. bulk. The analysis of stress distribution in the volume showed the von Mises stress concentration of 1.75 and stress concentration of 2.2 for the hydrostatic pressure. The observed stress concentration is high enough to cause localized plastic microdeformation, even when the polycrystalline aggregate is in the macroscopic elastic regime. The modeling of stresses and strains in polycrystalline materials can identify the microstructures (grain size distributions, texture) intrinsically susceptible to stress/strain concentrations and justify the correctness of applied stress state during the stress corrosion cracking tests. Also, it supplies the information necessary to formulate the local failure criteria and interpret the results of non-destructive stress measurements.

## INTRODUCTION

Intergranular cracks found on primary and secondary sides of steam generators with Alloy 600 tubing and other Alloy 600 components such as control rod drive and pressurizer nozzles are attributed to intergranular stress corrosion cracking (IGSCC). The process of intergranular stress corrosion in metal alloys is controlled by a combination of corrosive environment, applied (and/or residual) stress, and a susceptible microstructure. The microstructural characteristics often cited as affecting the susceptibility of nickel alloys to IGSCC in high temperature water are intergranular and intragranular carbides, grain boundary chromium depletion, impurity segregation, grain size, texture and cold work. There is experimental evidence that intergranular cracks in Alloy 600 primarily initiate and propagate at locations where a complex state of stress exist [1]. There is no experimental evidence regarding the mechanisms governing crack initiation; one can assume that the slip-related mechanism would be controlled by the deviatoric stresses (e.g., von Mises equivalent stress) which are responsible for material shearing, and the rupture-type mechanism would depend upon the hydrostatic stresses. The current understanding of the role of stress in crack initiation is such that the crack initiates at sites where a local stress concentration exists [1,3-4]. Grain boundaries, slip steps, and corrosion pits act as stress raisers and subsequently the localized plastic deformation leads to passive film rupture and to the nucleation of a crack [3-4]. In order to deform material

MASTER

## **DISCLAIMER**

**Portions of this document may be illegible  
in electronic image products. Images are  
produced from the best available original  
document.**

microplastically, the local stress must exceed the yielding stress. A polycrystal is an aggregate of randomly (or preferably) oriented grains, and under applied (and/or residual) stress inhomogeneous stress and strain distributions exist [5-8]. The local stress state is a superposition of three "types" of stresses: (1) the homogeneous stress state, which is averaged over the volume of many crystallites (called "macrostress"), (2) the inhomogeneous stress which varies within a crystallite due to its interactions with the neighboring grains ("microstress"), and (3) stress variations due to lattice defects (dislocations, vacancies, precipitates, etc.). The role of stress state on crack initiation is not clear; many SCC tests in high temperature water environments have resorted to specimens with complex stress states (i.e., reversed U-bends) to reduce test times. The influence of biaxial, triaxial, and cyclic stresses is yet to be determined [9].

This study is concerned with the distribution of stresses (superposition of the macroscopic and microscopic stresses) between individual randomly oriented crystallites in a "pure" microstructure (i.e., without impurities or precipitates) of a single phase alloy. The local concentrations of stresses at vertices in three-dimensional microstructures (grain boundary triple points at the surface in the two-dimensional case) and inside grains were studied as a function of the state of applied stress and grain orientation. The "pure" microstructure was selected for this study in order to determine the effect of the "intrinsic" properties of the microstructure (i.e., single crystal elastic anisotropy and grain topology) on the stress distribution.

### MODEL OF A POLYCRYSTALLINE AGGREGATE

A 3-dimensional microstructure was simulated using a Voronoi-Poisson tessellation generated within a unit cube (Fig. 1) following the algorithms described in Reference [10]. The simulated microstructure contained 500 grains and was shown to be topologically correct [11]. Each grain was divided into tetrahedral elements having a common vertex at the location of the original seed from which the grain had been grown. Such a division provided for 40-50 finite elements per grain [10]. The simulated microstructures had a random orientation of grains i.e., no crystallographic texture. Since the single crystal elastic constants for Alloy 600 were not available in the literature, they were estimated from the polycrystal elastic modulus [12] and the anisotropy factors for nickel and nickel superalloys [13-14]. The following single crystal elastic constants were recalculated:  $C_{11} = 232$  GPa,  $C_{12} = 148.0$  GPa, and  $C_{44} = 115.9$  GPa. The polycrystal elastic moduli for Alloy 600 estimated by the Kröner [15] averaging scheme were: Young's modulus  $E =$

203.9 GPa, shear modulus  $G = 78.0$  GPa, bulk modulus  $K = 176.0$  GPa, and Poisson ratio  $\nu = 0.307$ . The elastic moduli derived using the three-dimensional microstructural model and simulating uniaxial tensile and hydrostatic compression tests were:  $E = 206.2$  GPa and  $K = 176.0$  GPa showing an excellent agreement with the analytical predictions. The temperature dependence of elastic constants was not considered since there was no available data; limited experimental evidence shows that at 320°C (which is the operational regime for Alloy 600 tubing in nuclear power steam generators) the Young's modulus is lower by approximately 10% than the value at room temperature.

The boundary conditions were established in the following way. Recognizing that a IGSCC crack initiates at the surface where a plane state of stress is present, a biaxial pressure uniformly distributed on the cube faces was applied (Fig. 1). The two unloaded surfaces remained free. The analysis of residual stresses in Alloy 600 components (residual stresses are much higher than applied stresses) [16-17] showed that two cases of stress state can be considered as "typical": biaxial stress  $\sigma_x = \sigma_y$  and  $\sigma_y = 0.02\sigma_x$  ("almost" uniaxial tension). The numerical values were set as  $\sigma_x = 300$  MPa,  $\sigma_y = -300$  MPa in the first case and  $\sigma_x = 500$  MPa,  $\sigma_y = -10$  MPa in the second case, so that the average macroscopic von Mises stress was the same in both cases and equal to  $\sigma_m = 505$  MPa (which is approximately 70% of the tensile strength of a mill annealed Alloy 600 [18]). Such boundary conditions are also interesting from the theoretical standpoint, in that they allowed for the analysis of the stress distribution as a function of loading conditions, i.e., biaxial vs. uniaxial stress state. The stresses (von Mises, hydrostatic) at the vertices where the grains meet (4 grains meet at a common vertex in the bulk material, 3 grains meet at the surface) were calculated using MSC/NASTRAN V.66 finite element package.

### DISTRIBUTION OF STRESSES IN A POLYCRYSTALLINE AGGREGATE

The stresses were calculated at vertices where four grains meet (three grains at the surface) and in the grain interiors at the points corresponding to the location of the original "seeds". Two scalar stresses were calculated: von Mises stress (second invariant of the deviator stress tensor) as relevant to the slip-type mechanism of crack initiation, and hydrostatic stress (one third of the first invariant of the stress tensor) as relevant to the hydrogen embrittlement type of material damage.

Fig. 2-5 show the distributions of von Mises and hydrostatic stresses on the free surface and their dependence on the loading mode and grain orientations. Fig. 2 shows that the hydrostatic stress distribution on the surface depends strongly on grain

orientations; as the orientation of grains changes the stress distribution changes also due to different elastic interactions between the grains. However, the microstructural features, such as small grains (for example the grain marked as A in Fig. 2 and 3) with sharp shapes, act as stress raisers, regardless of their own orientation and the orientations of the adjacent grains. The current research for three dimensional arrangements of grains having a two parameter gamma distribution of volumes shows that small grains are more effective stress raisers than large grains. The stress distribution in a grain results from the interactions with all neighboring grains (14 on average for a single phase material); however, the smaller grains have fewer faces (and neighbors) than the bigger ones, with the minimum number of four. Therefore, the effect of the potential extreme contact stresses with one neighbor is more pronounced in the case of small grains. The same observations apply to von Mises stresses (Fig. 3): stress distribution is dictated by the microstructure (grain topology) and the grain orientations. The effect of loading mode on von Mises stress distribution on the surface is not significant. As seen in Fig. 5, the character of von Mises stress distribution is very similar for the uniaxial and biaxial modes of loading. The distribution of hydrostatic stress is for the most part not strongly dependent on the loading mode (Fig. 4) except for the locations where small grains with irregular shapes (e.g., grains marked as B and C in Fig. 4) act as stress raisers; change of loading from uniaxial to biaxial causes an abrupt change in hydrostatic pressure. Therefore, if the local damage criterion based on von Mises or hydrostatic stresses was applicable to Alloy 600, a uniaxial SCC test would not reflect the stress effects due to actual multiaxial loading of a component. The elastic stress concentration at grain boundary vertices was found to be 1.7 for the hydrostatic pressure and 1.5 for the von Mises stresses in Alloy 600.

The distribution of elastic stresses and strains in the grain interiors (between grain portions represented by finite elements) was found to be a normal (Gaussian) distribution. Figure 6 shows the distribution of the hydrostatic and von Mises strains. The strain/stress distributions on cube surfaces (on planes defined as  $x,y,z = 0$  or 1 in Fig. 1) and in the cube interior are very similar showing that there is no surface effect on the elastic stress/strain distribution. The mean value of stresses/strains (0 in units of standard deviation as shown in Fig. 5) corresponds approximately to the value of the applied macroscopic stress. The standard deviation  $\sigma$  depends on the elastic anisotropy of the material [19]; the higher the elastic anisotropy the higher the standard deviation. For Alloy 600 (Zener anisotropy factor  $A=2.76$ ) the standard deviation of von Mises stress was found to be 25% of the applied stress and

for hydrostatic pressure the standard deviation was 40% of applied stress. Therefore, from the properties of a normal distribution it follows that 68% of the material volume is subjected to the stress  $\sigma_m \pm \sigma$  ( $\sigma_m$  is the mean applied stress), 99.7% of the volume is subjected to  $\sigma_m \pm 3 \sigma$  etc. In terms of the extreme values of stress, 0.3% of the material (grains) is subjected to stress 2.2 times higher than the applied hydrostatic stress and 1.75 times higher than the applied von Mises stress.

Non-destructive techniques such as neutron or x-ray diffraction used for residual stress measurement or for monitoring of applied stresses determine the macroscopic stress averaged over thousands of grains. The experimental data combined with modeling can provide information regarding the stress/strain distribution for a given material. The knowledge of local stress concentration i.e. the magnitude and location of maximum stress can be very useful while using the local fracture criteria (which are usually orientation dependent) for crack initiation and propagation [20].

## CONCLUSIONS

The stress distribution in a polycrystalline material (Alloy 600) was studied using a topologically correct microstructural model. The distributions of von Mises and hydrostatic stresses at the grain vertices, which could be important factors when studying IGSCC initiation, were analyzed as a function of microstructure, grain orientations and loading conditions. The grain size, shape, and orientation had a more pronounced effect on stress distribution than the loading conditions. The stress concentration factor was higher for hydrostatic stress (1.7) than for von Mises stress (1.5) for Alloy 600. The stress/strain distribution in the volume (grain interiors) is a normal distribution and does not depend on the location of the studied material volume i.e., surface vs. bulk. The analysis of stresses distribution in the volume showed the von Mises stress concentration of 1.75 and stress concentration of 2.2 for the hydrostatic pressure. The observed stress concentration is high enough to cause localized plastic microdeformation, even when the polycrystalline aggregate is in the macroscopic elastic regime. The modeling of stresses and strains in polycrystalline materials can identify the microstructures (grain size distributions, texture) intrinsically susceptible to stress/strain concentrations and justify the correctness of applied stress state during the SCC tests. Also, it supplies the information necessary to formulate local failure criteria and interpret the results of non-destructive stress measurements.

## ACKNOWLEDGEMENTS

This project was supported by the Electric Power Research Institute, Palo Alto, California. One of the authors (KJK) was partially sponsored by the U. S. Department of Energy, Assistant Secretary for Energy Efficiency and Renewable Energy, Office of Transportation Technologies, as part of the High Temperature Materials Laboratory User Program under contract DE-AC05-84OR21400, managed by Martin Marietta Energy Systems, Inc.

## REFERENCES

1. N. TOTSUKO, E. LUNARSKA, G. CRAGNOLINO, and Z. SZKLARSKA-SMIALOWSKA, "Effect of Hydrogen on the Intergranular Stress Corrosion Cracking of Alloy 600 in High Temperature Aqueous Environments," *Corrosion* 43 (8) (August 1987) 505.
2. T.S. BULISCHECK and D. VAN ROOYEN, "Effect of Environmental Variables on the Stress Corrosion Cracking of Inconel 600 Steam Generator Tubing," *Nuclear Technology* 55 (Nov. 1981) 383.
3. H. VEHOFF, H. STENZEL, and P. NEUMANN, "Experiments on Bicrystals Concerning the Influence of Localized Slip on the Nucleation and Growth of Intergranular Stress Corrosion Cracks," *Z. Metallkde.* 78 (8) (1987) 550.
4. Y.S. GARUD and A.R. McILREE, "Intergranular Stress Corrosion Cracking Damage Model: An Approach and its Development for Alloy 600 in High-Purity Water," *Corrosion* 42 (2) (Feb. 1986) 99.
5. YU. V. GRINYAER and V.E. PANIN, "Stress State in Elasticity Loaded Polycrystal," *Izvestiya Vysshikh Uchebnykh Zavedenii, Fizika* 12 (Dec. 1978) 95.
6. K. HASHIMOTO and H. MARGOLIN, "The Role of Elastic Interaction Stresses on the Onset of Slip in Polycrystalline Alpha Brass - I. Experimental Determination of Operating Slip Systems and Qualitative Analysis," *Acta Metall.* 31 (5) (1983) 773.
7. K. HASHIMOTO and H. MARGOLIN, "The Role of Elastic Interaction Stresses on the Onset of Slip in Polycrystalline Alpha Brass - II. Rationalization of Slip Behavior," *Acta Metall.* 31 (5) (1983) 787.
8. V.E. PANIN, YU. V. GRINYAER, T.F. ELSUKOVA, K.P. ZHUKOVA, and E.M. NOVOSELOVA, "Nonuniformity of the Stress Distribution and Motion of Grains as a Whole in a Deformable Single Crystal," *Sov. Phys. Dokl.* 34 (11) (Nov. 1989) 1034.
9. P. COMBRADE, "The Role of Surface Films on the Control of Alloy 600 Corrosion in PWR Reactors--No Results, A Few Comments, A Lot of Questions," presented at EPRI Alloy 600 Expert Meeting, Airlie, VA, 6-9 April 1993.
10. S. KUMAR, Ph.D. Thesis, The Pennsylvania State University (1992).
11. S. KUMAR, S.K. KURTZ, J.R. BANAVAR, and M.G. SHARMA, "Properties of a Three-Dimensional Poisson-Voronoi Tessellation: A Monte Carlo Study," *J. Stat. Physics* 67 (3/4) (May 1992) 523.
12. W. WESTON, H. LEDBETTER, and E. NAIMON, "Dynamic Low-Temperature Elastic Properties of Two Austenite Nickel-Chromium-Iron Alloys," *Mat. Sci. Eng.* 20 (1975) 185.
13. D. DANDEKAR and A. MARTIN, "Single Crystal Elastic Constants of Two Nickel Based Superalloys," *J. Mat. Sci. Letters* 8 (1989) 1172.
14. H.A. KUHN and H.G. SOCKEL, "Comparison Between Experimental Determination and Calculation of Elastic Properties of Nickel-Base Superalloys Between 25 and 1200°C," *Phys. Stat. Sol. (a)* 110 (1988) 449.
15. E. KRÖNER, *Z. Phys.* 151 (1958) 504.
16. C.O. RUUD et al., "Residual Stress Analysis of Alloy 600 U-Bends, RUBs, and C-Rings," EPRI Report, 1991.
17. C.O. RUUD et al., "Residual Stresses in Roller Expanded Heat Exchanger Tube Transitions," EPRI Report, 1993.
18. EPRI report NP-6705-SD, "Measurement of Surface-Induced Microplasticity in Alloy 600 C-Rings," (1990) p. 2.
19. L.D. DIKUSAR, E.F. DUDAREV, and V.E. PANIN, "Statistical Theory of the Microdeformations of Polycrystals. I." *Izv. Vyssh. Uchebn. Zaved., Fizika* 8 (August 1971) 96.
20. J.GIL SEVILLANO and A. MARTIN MEIZOSO, "The Influence of Texture on Fracture," *Eight International Conference on Textures of Materials (ICOTOM8)*, ed. J.S. KALLEND and G. GOTTSSTEIN (Warrendale, PA: TMS, 1988) p. 897.

## DISCLAIMER

This report was prepared as an account of work sponsored by an agency of the United States Government. Neither the United States Government nor any agency thereof, nor any of their employees, makes any warranty, express or implied, or assumes any legal liability or responsibility for the accuracy, completeness, or usefulness of any information, apparatus, product, or process disclosed, or represents that its use would not infringe privately owned rights. Reference herein to any specific commercial product, process, or service by trade name, trademark, manufacturer, or otherwise does not necessarily constitute or imply its endorsement, recommendation, or favoring by the United States Government or any agency thereof. The views and opinions of authors expressed herein do not necessarily state or reflect those of the United States Government or any agency thereof.

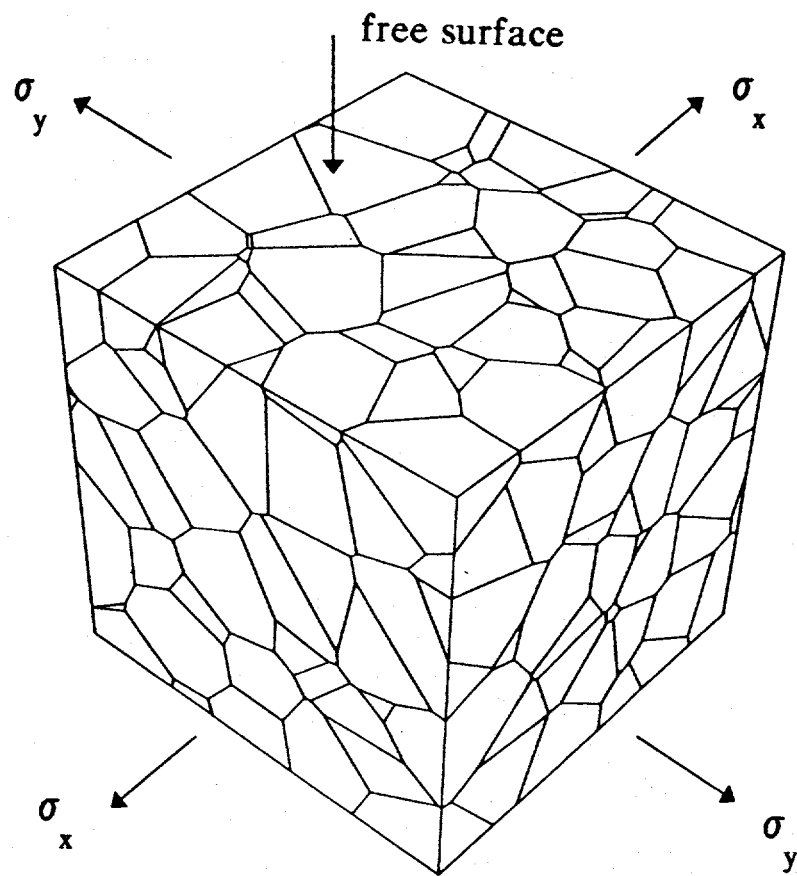


FIGURE 1. UNIT CUBE SHOWING GRAIN BOUNDARIES AND LOADING CONDITIONS.

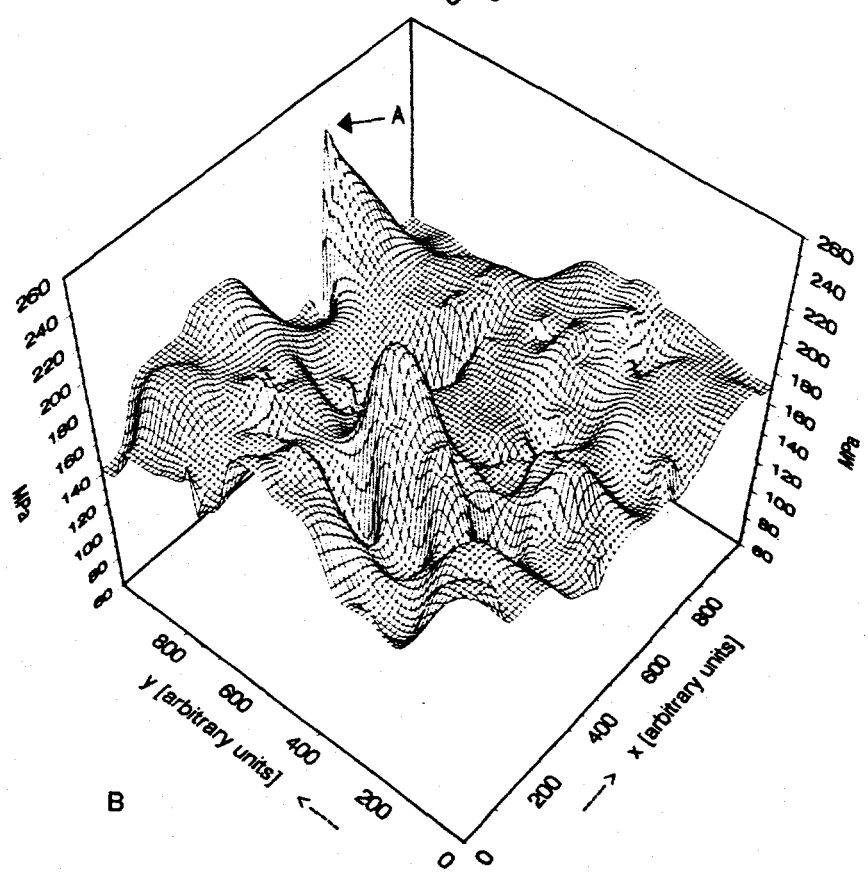
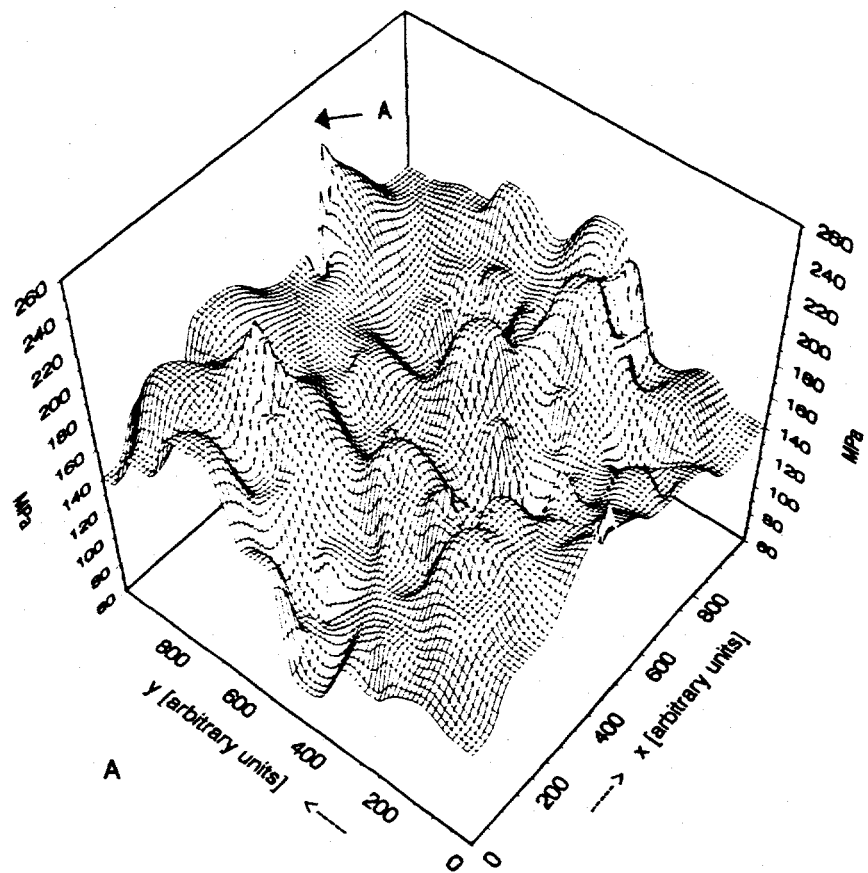


FIGURE 2. DISTRIBUTION OF HYDROSTATIC STRESSES ON THE FREEE SURFACE. UNIAXIAL LOADING CONDITIONS. (A) FIRST SET OF GRAIN ORIENTATIONS, (B) SECOND SET OF GRAIN ORIENTATIONS.

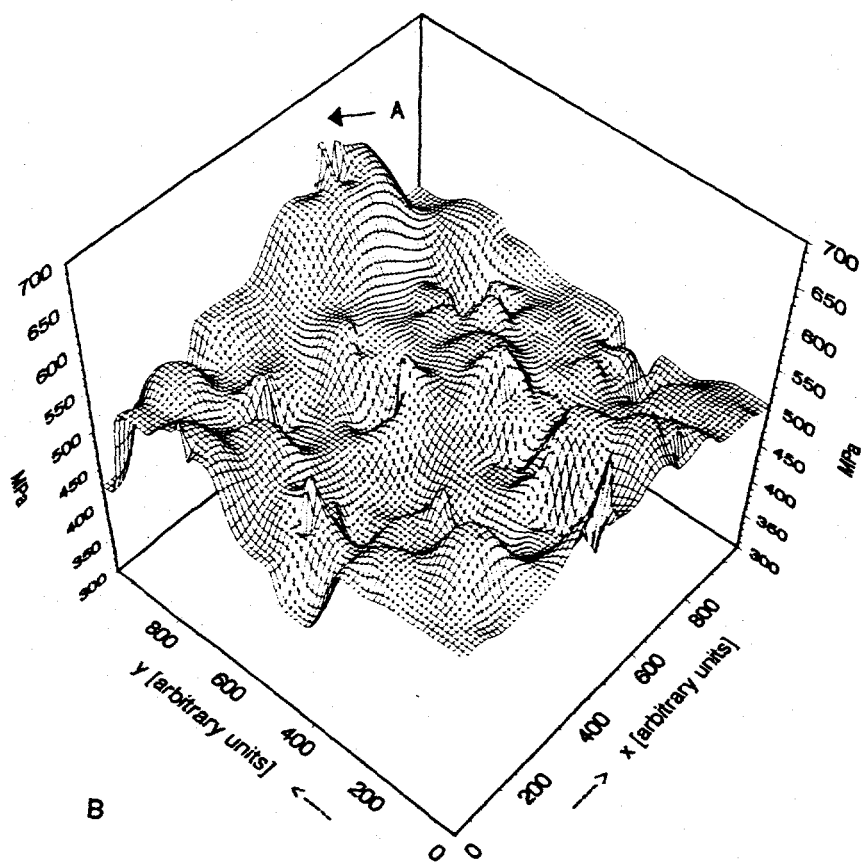
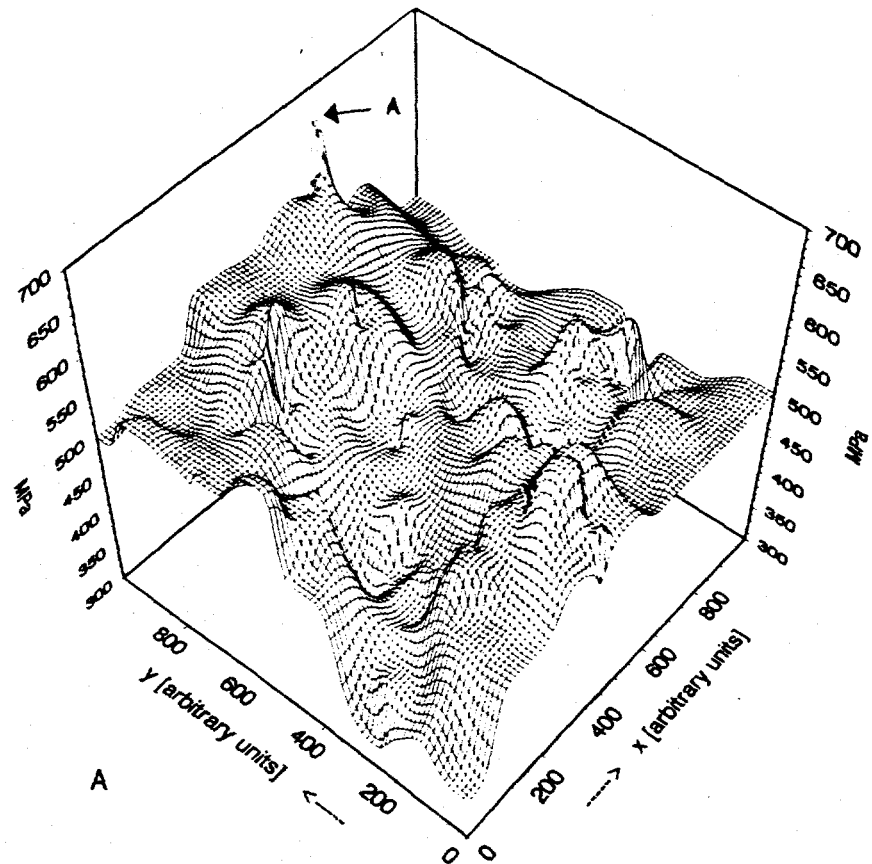
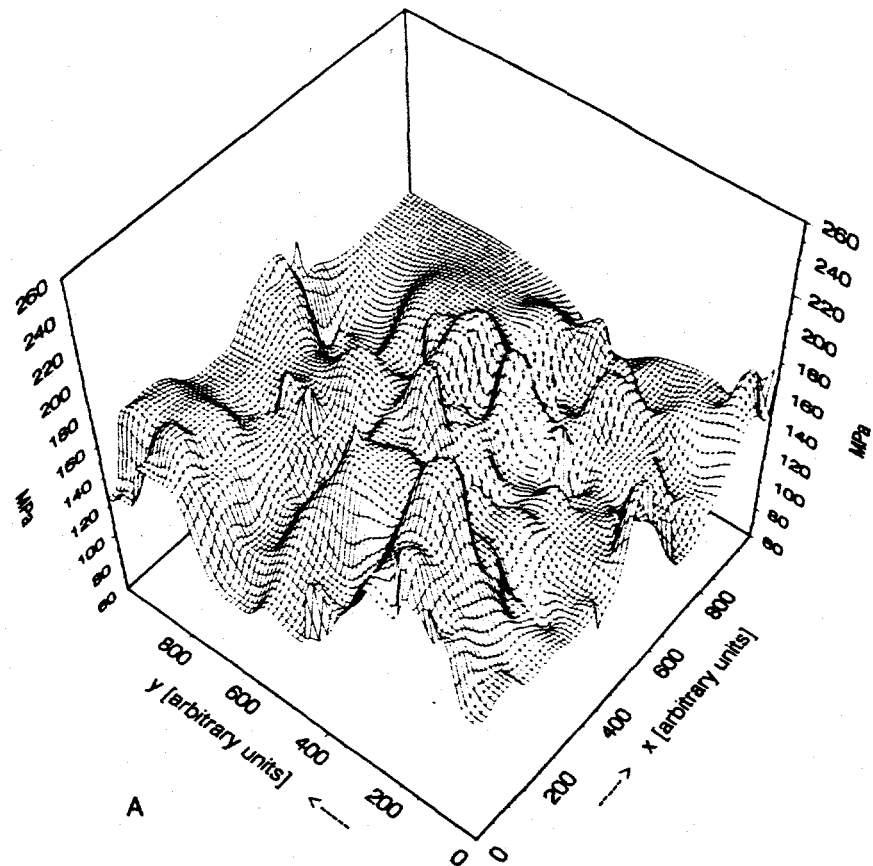
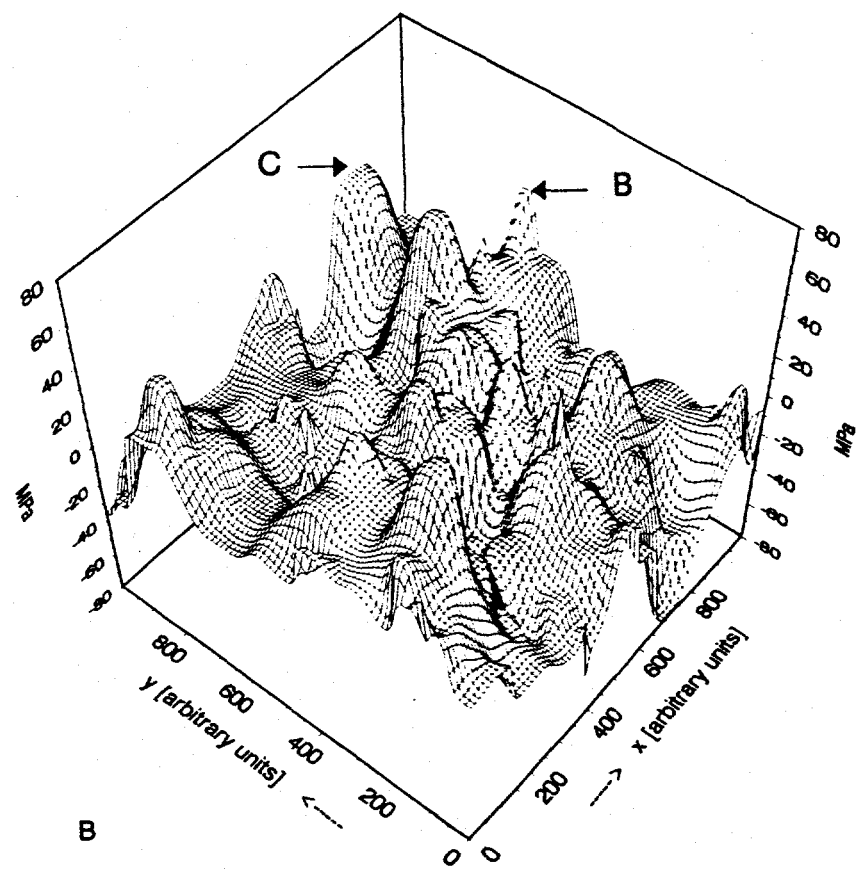


FIGURE 3. DISTRIBUTION OF VON MISES STRESSES ON THE FREE SURFACE. UNIAXIAL LOADING CONDITIONS. (A) FIRST SET OF GRAIN ORIENTATIONS, (B) SECOND SET OF GRAIN ORIENTATIONS.



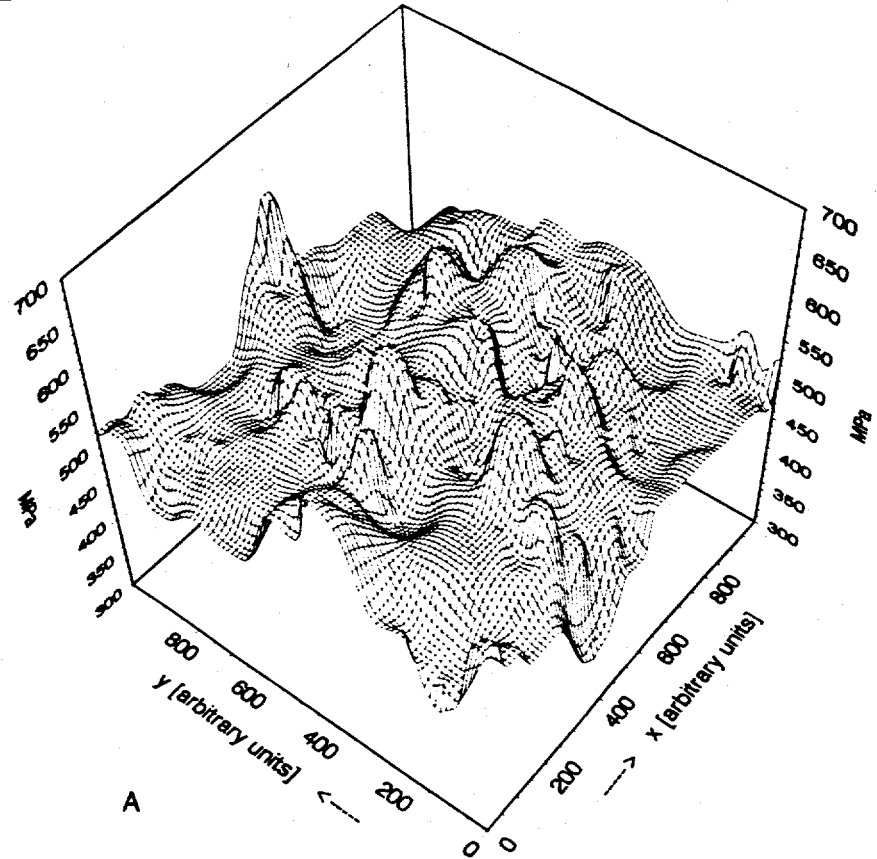
A



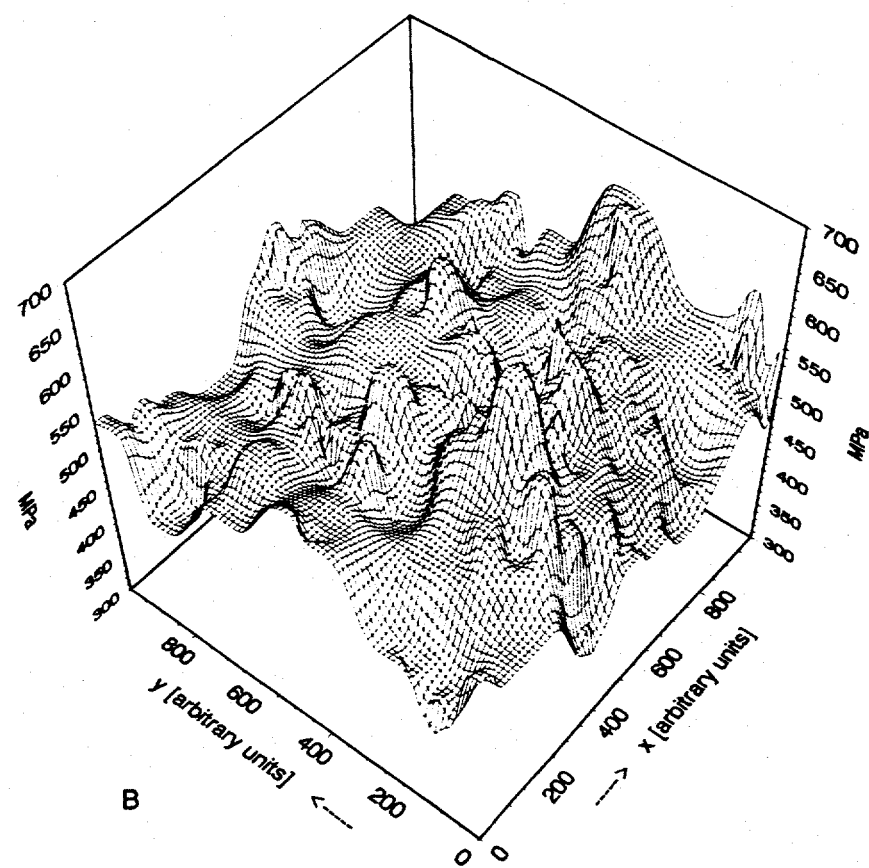
B

C

FIGURE 4. DISTRIBUTION OF HYDROSTATIC STRESSES ON THE FREE SURFACE. LOADING CONDITIONS (A) UNIAXIAL, (B) BIAXIAL.

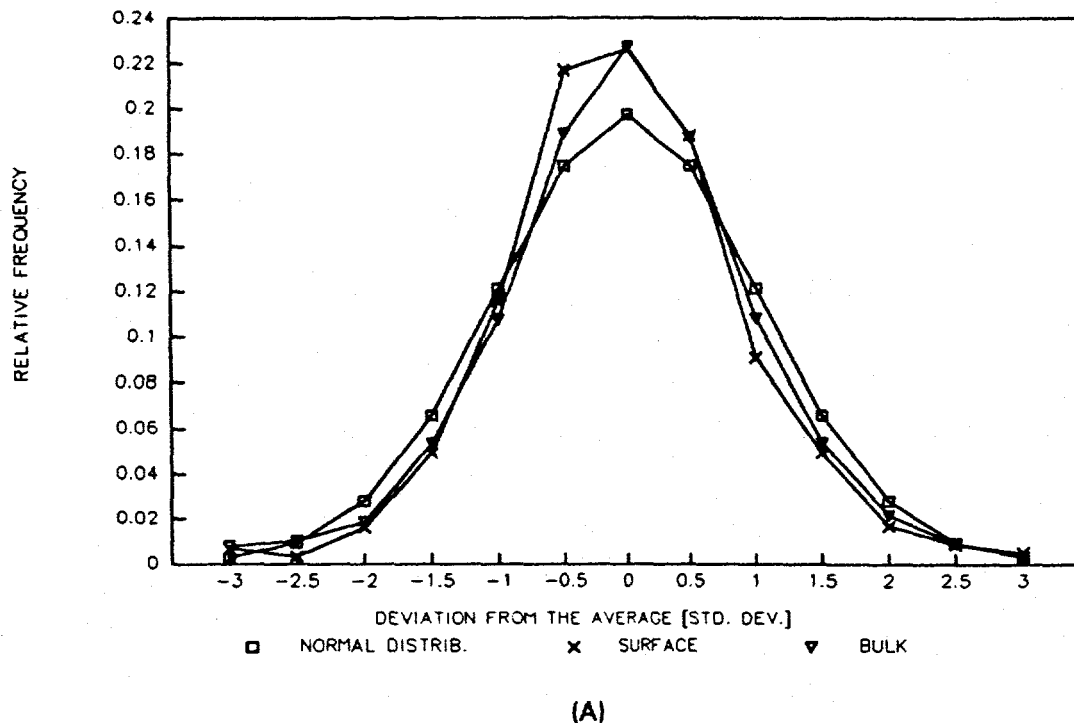


A

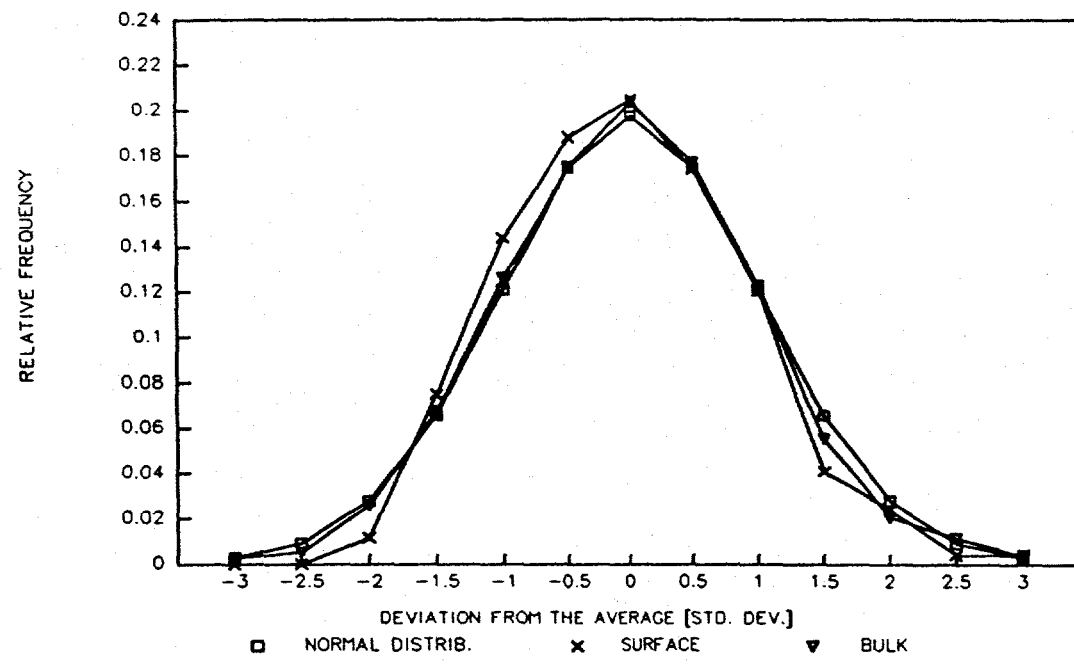


B

FIGURE 5. DISTRIBUTION OF VON MISES STRESSES ON THE FREE SURFACE. LOADING CONDITIONS (A) UNIAXIAL, (B) BIAXIAL.



(A)



(B)

FIGURE 6. DISTRIBUTION OF HYDROSTATIC STRAINS (A) AND VON MISES STRAINS (B) ON THE SURFACE AND IN THE BULK OF ALLOY 600.